Turkish Journal of Engineering & Environmental Sciences

http://journals.tubitak.gov.tr/engineering/

Research Article

Turkish J Eng Env Sci
(2013) 37: 91 – 99

doi:10.3906/muh-1201-6

Enhancing purification of an azo dye solution in nanosized zero-valent iron-ZnO photocatalyst system using subsequent semibatch packed-bed reactor

Ali KHANI*, Mahmoud Reza SOHRABI, Morteza KHOSRAVI, Mehran DAVALLO
Faculty of Chemistry, North Tehran Branch, Islamic Azad University, Tehran, Iran

Received: 08.01.2012 • **Accepted:** 21.11.2012 • **Published Online:** 04.03.2013 • **Printed:** 01.04.2013

Abstract: In this work, simultaneous synthesis–immobilization of nano zero-valent iron (reductive catalyst) and nano ZnO (photocatalyst) on perlite as a suitable bed (nZVI-P and nZnO-P) was done. Three processes (reduction, oxidation, and reduction–oxidation) were evaluated for removal of azo dye C.I. acid orange 7 (AO7) from aqueous solution in a semibatch packed-bed reactor. Our results show that AO7 was successfully removed, synchronously in terms of its total color and total organic carbon, using integrated innovative technology by coupling the reduction system (nZVI-P) with the photodegradation process (nZnO-P). Thus, the coupling provided a superior solution for dye wastewater treatment. The kinetic results confirmed the pseudo-first-order model for the Re–Ox process in all initial concentrations of the dye on the basis of P.

Key words: Nanocatalyst, ZnO, ZVI, degradation, azo dye, water treatment

1. Introduction

Wastewaters from textile, paper, and some other industries contain residual dyes, which are not readily biodegradable. Adsorption and chemical coagulation processes are 2 common techniques of wastewater treatment. However, these methods merely transfer dyes from the liquid to the solid phase, causing secondary pollution and requiring further treatment. Advanced oxidation processes (AOPs) are alternative techniques for removing dyes and many other organics in wastewater and effluents. These processes generally involve UV/H_2O_2, UV/O_3, or UV/Fenton's reagent for the oxidative degradation of contaminants. Semiconductor photocatalysis is another developed AOP, which can be conveniently applied to remove different organic pollutants (Khodja et al., 2001; Chakrabarti and Dutta, 2004; Daneshvar et al., 2004; Kandavelu et al., 2004).

In recent years, the uses of zero-valent iron, Fe0 (ZVI), for the treatment of toxic chemicals in waters have received wide attention (Kanel et al., 2005; Karri et al., 2005). ZVI is a strong reducing agent; it is cheap and easy to produce. It has already been proven effective in reducing chlorinated solvents including chlorinated organics (Schrick et al., 2002; Zhang, 2003), nitroaromatic compounds (Agrawal and Tratnyek, 1996; Devlin et al., 1998), pesticides (Antoine, 2001), nitrate (Huang et al., 1998), chlorinated organic compounds (Chang and Cheng, 2006; Xiong et al., 2007), and metal ions such as Cr(VI) (Ponder et al., 2000; Hu et al., 2005). Lin and Weng (2008) studied the reductive degradation of azo dye AB24 by nanosized/microsized zero-valent iron.

Although ZVI reduction technology was proven to be very effective on decolorization, it is very limited for mineralizing the organic compound residues (Chang et al., 2006; Shu et al., 2009). The ZnO/UV process

*Correspondence: a.khani59@yahoo.com

for textile effluents simultaneously gives excellent efficacy for both decolorization and mineralization. However, it not only consumes high electrical power but also results in lower UV light efficiency due to high absorbance by dye wastewater. Thus, integration of 2 processes using the initial ZVI for high color removal followed by the nano ZnO/UV oxidation process (nZVI.ZnO-P) for full mineralization was proposed to obtain not only complete decolorization and mineralization but also savings in time and energy.

The key to the problem of industrializing the technology seems to be simple, with low-cost immobilization of catalysts on solid media (Machado and Santana, 2005; Medina-Valtierra et al., 2005; Cheng et al., 2007; Gong et al., 2009).

In this study, the perlite was selected as a base for nanoparticles of ZnO and ZVI for its merits including high porosity, low density, natural abundance, the absence of toxicity, and low cost (Erdem et al., 2007; Hosseini et al., 2007).

The proposed technology employs reductive decolorization by nZVI, sequentially connected to the oxidative nZnO/UV process for mineralization of organics. In this work, all experiments were performed using tow semibatch packed-bed reactors connected to an online sampling UV-Vis spectrophotometer.

2. Experimental

The expended perlite (EP) used in the present study was obtained from Goohar Sahand Co. (Iran). The chemical composition and properties of the EP are shown in Table 1. C.I. acid orange 7 (AO7) as a pollutant was purchased from Boyakhsaz Co. (Iran). $NaBH_4$, $FeCl_3.6H_2O$, zinc nitrate, NaOH, and H_2SO_4 were purchased from Merck (Germany). Deionized distilled water was used in all experiments and all experiments were repeated twice (variance (σ^2) = 0.0021).

Table 1. Chemical composition and properties of expanded perlite.

Constituents	Percentage (wt%)
SiO_2, Al_2O_3, K_2O, CaO, Na_2O, Fe_2O_3, MgO, MnO_2	81, 11.4, 4.3, 0.9, 0.8, 0.7, 0.6, 0.2, 0.1
Properties	
Color	White
pH	7
Specific area	5.3 m^2 g^{-1}
Melting point	1300 °C
Density	3 g cm^{-3}
Granule shape	Globular
Solubility in water	Not soluble

2.1. Preparation of nanocatalyst immobilized perlite

2.1.1. nZnO-perlite

The nanoparticles of ZnO supported on perlite (nZnO-P) were prepared from pyrolysis of adsorbed zinc nitrate on perlite. A solution of $Zn(NO_3)_2$ (0.2 M) was stirred with perlite (4 g) in deionized water for 30 min until the zinc nitrate was adsorbed on the expended perlite. The perlite was then filtered and washed with deionized water and heated to 400 °C for 1 h in an air oven for pyrolysis of zinc nitrate to ZnO.

2.1.2. nZVI-perlite

The nanosized zero-valent iron (nZVI) particles were chemically synthesized (Shu et al., 2007). Next, a 250-mL solution of $FeCl_3.6H_2O$ (0.2 M) was stirred with perlite (4 g) in deionized water for 20 min until ferric chloride was adsorbed on the expended perlite. The borohydride solution (1 M and approximately 100 mL) was then added dropwise to the aqueous Fe^{3+} and perlite mixture at room temperature while stirring thoroughly using a magnetic mixer. The black solid particles of nZVI appeared immediately following the addition of the first drop of $NaBH_4$ solution. After the full addition of the borohydride solution, the mixture was thoroughly stirred for a further 10 min. The reduction of ferric iron by borohydride ions can be represented according to the following equation:

$$3Fe^{3+} + 6BH_4^- + 18H_2O \longrightarrow 3Fe^0 + 6B(OH)_3 + 21H_2. \quad (1)$$

To evaluate the supporting treatment, nZnO-P and nZVI-P particles were washed twice with deionized water and then dried.

2.2. Experimental set up

In order to assess the removal of AO7 and the kinetics study, 3 processes were used: 1) integrated Re–Ox (nZVI.ZnO-P), 2) reduction (nZVI-P), and 3) oxidation (nZnO-P) systems. The system included the following instruments: the packed-bed tubular reactor connected to an online sampling UV-Vis spectrophotometer (UV-Vis spectrophotometer, a designed absorption cell), peristaltic pump, solution reservoir, and quartz-covered UV-C lamp (used in nZnO system, 8 W, Philips, light intensity of 0.4 klx measured with a lux meter, Leybold-Heraeus), as shown in Figure 1.

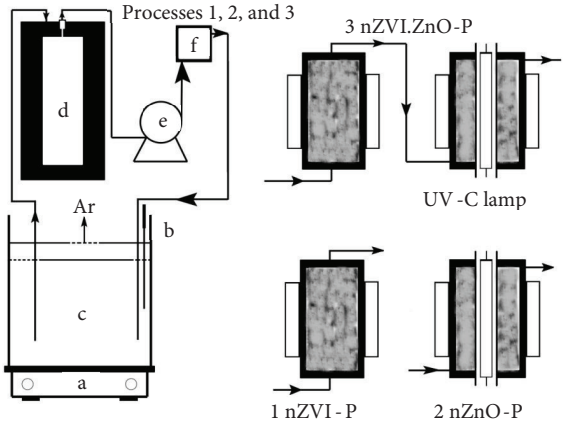

Figure 1. The schematic diagram of the experimental apparatus: (a) magnetic stirred hot plate, (b) thermometer, (c) solution tank, (d) UV-Vis spectrophotometer, (e) peristaltic pump, and (f) processes used: (1) nZVI-P, length = 30 cm, D = 5 cm; (2) nZnO-P, length = 30 cm, D_{out} = 5.5 cm, D_{in} = 2.5 cm; and (3) integrated system, length = 15 cm.

2.3. Procedures

To remove AO7, a solution containing known concentrations of dye was prepared and then 1 L of the prepared solution was transferred to a Pyrex beaker and agitated with a magnetic stirrer during the experiment. The solution was pumped with a peristaltic pump (Heidolph, PD 5001) through the circular packed-bed photoreactor. The solution temperature was adjusted with a water cooling system installed on the reactor wall, and for

photocatalytic reaction, the lamp was switched on to initiate the reaction. The concentration of the dye solution was determined with an online sampling spectrophotometer system (UV-Vis spectrophotometer, PerkinElmer 550 SE) at $\lambda_{max} = 485$ nm. The degree of removal of AO7 was calculated at different time intervals using the equation given below.

$$X = \frac{C_0 - C_t}{C_0} \tag{2}$$

Here, X is the degree of decolorization, C_0 is the initial concentration of AO7, and C_t is the concentration of AO7 at time t.

3. Results and discussion

3.1. XRD and SEM analysis

The results from the XRD analysis are shown in Figure 2. Figure 3 shows SEM images of the surface of the prepared catalyst. Figure 2 indicates that the average particle size is about 40 nm. The image of the perlite surface shows high porosity of perlite granules as a good support for the catalysts.

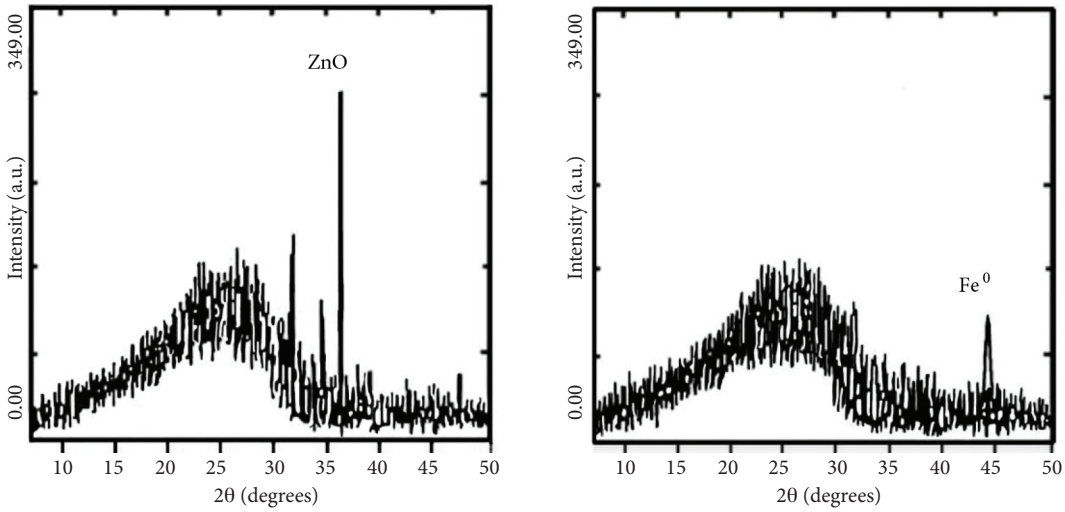

Figure 2. XRD patterns of ZnO and ZVI nanoparticles immobilized on the expanded perlite.

3.2. Comparative study

To evaluate the proposed integrated system (nZVI.ZnO-P), an experiment under basic conditions (initial concentration of AO7 = 125 mg L^{-1}, weight of catalyst (nZnO, nZVI, and nZVI.ZnO-P) = 55 g, pH 7, 25 °C, flow rate of solution = 150 mL min^{-1}, granule size of catalyst = 4 mm, volume of solution = 1 L, and reaction time = 90 min) was designed in order to measure the degree of decolorization of AO7 (X) under 3 processes: reduction with nano ZVI-perlite (nZVI-P), photooxidation with nano ZnO-perlite/UV (nZnO-P), and treatment with an integrated system (nZVI.ZnO-P), which are all shown in Figure 4.

As can be seen from Figure 4, the integrated system showed the highest decolorization efficiency (92%). The decolorization efficiencies for the nZnO-P and nZVI-P systems were 32% and 77% after 90 min, respectively.

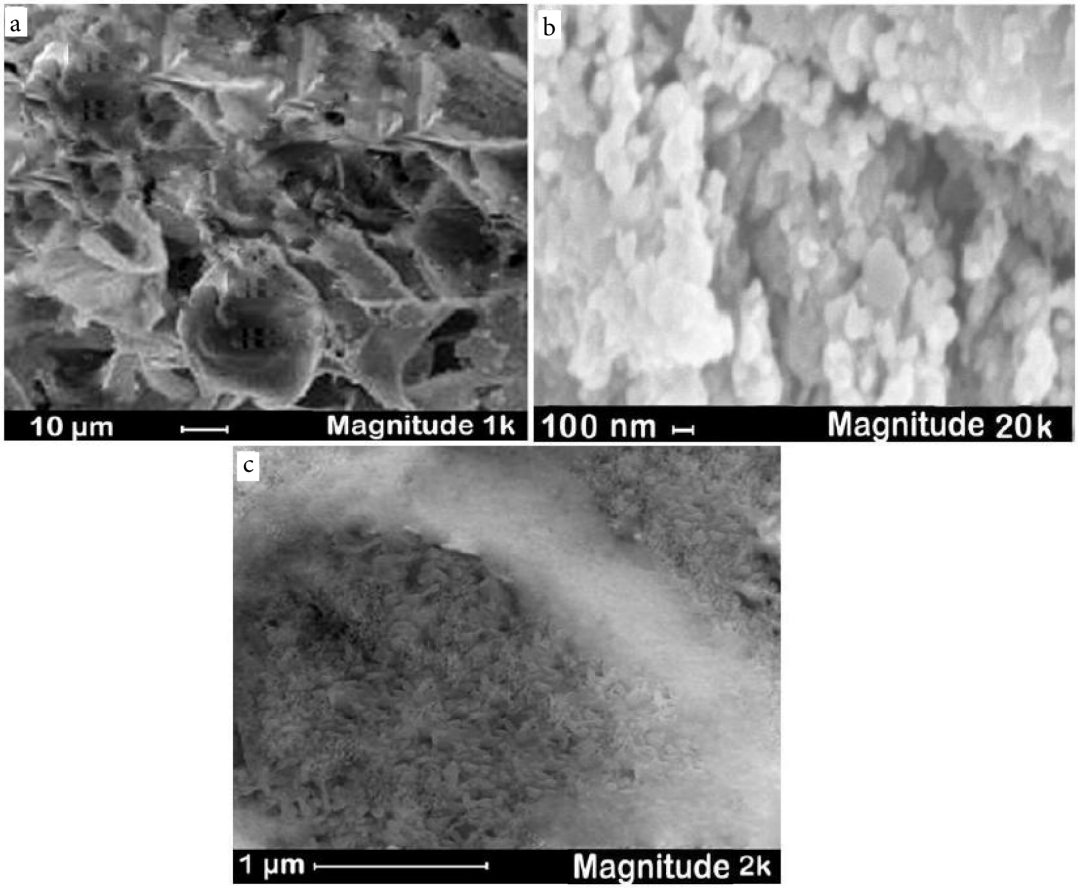

Figure 3. SEM images of (a) perlite, (b) nZVI-P, and (c) nZnO-P.

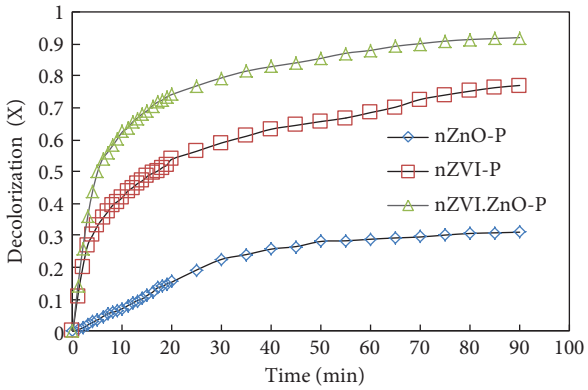

Figure 4. The decolorization of AO7 under 3 processes at basic conditions.

3.3. Effect of initial dye concentration

To study the effect of initial dye concentration on the decolorization efficiency of AO7, the experiments were conducted with initial dye concentrations varying from 75 to 175 mg L^{-1}. The decolorizations of initial dye concentrations by different systems are shown in Figure 5. The decolorization efficiency of AO7 by both the nZVI-P and nZVI.ZnO-P systems increased with an increase in dye concentration, with the integrated

system (nZVI.ZnO-P) showing much higher decolorization efficiency (97%) than the nZVI-P system (86%) at an initial dye concentration of 175 mg L^{-1}. In contrast, the nZnO-P system showed a different trend, in that decolorization efficiency decreased with an increase in dye concentration. This may be attributed to several factors. At high dye concentrations, the adsorbed dye molecules may occupy all the active sites of the photocatalyst surface, and this leads to the decrease in degradation efficiency. This means that as the concentration of the dye increases, more and more molecules of the dye get adsorbed on the surface of the photocatalyst. Therefore, requirements of the reactive species ($^{\bullet}OH$ and $^{\bullet}O_2^-$) for the degradation of the dye also increase. However, the formation of $^{\bullet}OH$ and $^{\bullet}O_2^-$ on the catalyst surface remains constant for a given light intensity, catalyst loading, and duration of irradiation. Hence, the available hydroxyl radicals are inadequate for the degradation of the dye at high concentrations. Consequently, the degradation efficiency of the dye decreases as the concentration increases (Khataee et al., 2001; Bahnemann et al., 2007; Kesraoui-Abdessalem et al., 2008). In addition, an increase in the substrate concentration can lead to the generation of intermediates, which may adsorb on the surface of the catalyst. Slow diffusion of the generated intermediates from the catalyst surface can result in the deactivation of active sites of the photocatalyst and, consequently, a reduction in the degradation efficiency. In contrast, at low concentrations, the number of the catalytic sites will not be a limiting factor and the rate of degradation is proportional to the substrate concentration (Selvam et al., 2007). Another reason may be the absorption of light photons by the dye itself, leading to a lesser availability of photons for hydroxyl radical generation (Damodar and Swaminathan, 2007; Khataee et al., 2011).

In the nZVI-P system, the effect of the initial dye concentration can be explained by the chemical structure of the dyes. If the chemical structure of a dye such as AO7 is simple, it is possible that increasing the initial dye concentration would have a positive effect on removal efficiency (Rahmani et al., 2010).

3.4. Evaluation of degradation efficiency in the systems used

Integration of nZVI reduction with the nZnO/UV oxidation process leads to a complete degradation and mineralization of the AO7 solution. Figure 6 shows that the nZVI.ZnO-P process can remove effectively not only color but also total organic carbon (TOC). The nZVI reduction process results in high dye removal but low TOC removal. Thus, connecting the nZVI reduction with the nZnO-P photooxidation process was proposed for rapid dye molecule degradation to remove color and mineralization of the residual organic compounds to reduce the TOC.

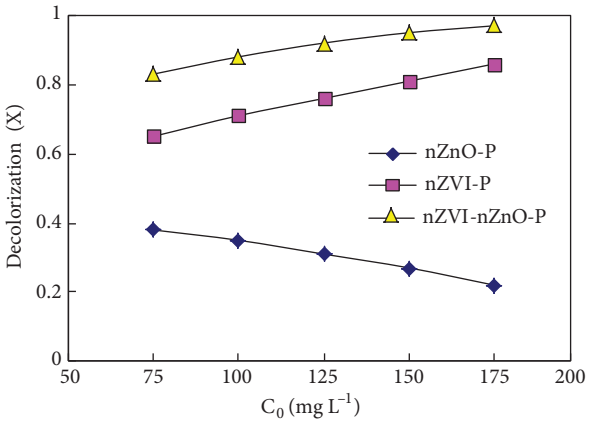

Figure 5. Effect of initial dye concentration on decolorization of AO7.

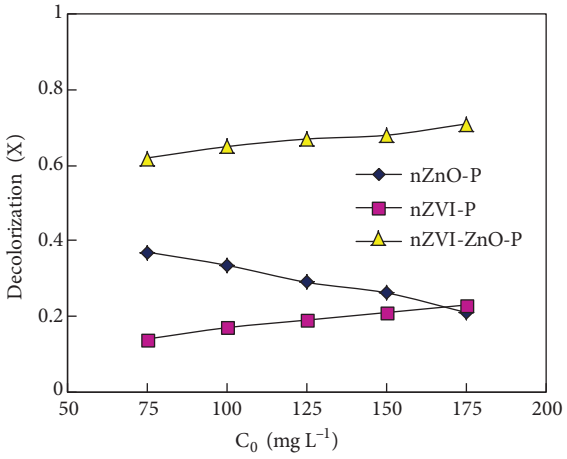

Figure 6. Comparison of degradation efficiency under 3 processes used at various initial concentrations.

3.5. Kinetics study

The following pseudo-first-order reaction model can be used to describe the rate phenomena observed for a nZVI.ZnO-P system.

$$r_R = \frac{-dC_R}{dt} = \frac{k_r K C_r}{1 + K R_R} \tag{3}$$

Here, r_R is the rate of reaction (degradation of solute R), C_R is the solute concentration, t is the time of the reaction, and k_r and K are the reaction and adsorption constants associated with the solute, respectively. When the concentration is low, KC_R is often negligible and the apparent reaction rate will follow a pseudo-first-order model. Integration of the equation under this assumption with boundary conditions of $C_R = C_{R0}$ at $t = 0$ yields:

$$-\ln\left(\frac{C_R}{C_{R0}}\right) = k_{app} t, \tag{4}$$

where C_{R0} is the initial substrate concentration and k_{app} is the apparent first-order reaction rate. The photocatalytic reactions in many cases show this behavior (Daneshvar et al., 2004; Daneshvar et al., 2007c; Khani et al., 2012). A better criterion is to introduce a parameter known as normalized percent deviation, the lowest average absolute percent deviation (%D), or in some studies, the percent relative deviation modulus, P, given by the following equation (Daneshvar et al., 2007a; Daneshvar et al., 2007b):

$$P = \frac{100}{N} \sum \frac{|y_{\exp} - y_{pred}}{y_{\exp}}, \tag{5}$$

where y_{exp} is the experimental y at any x, y_{pred} is the corresponding predicted y according to the equation under study with best fitted parameters, and N is the number of observations. It is clear that the lower the P value, the better the fit. The fit is accepted to be good when P is below 5. The linear trend observed in these plots proves that the photocatalytic degradation of AO7 at the conditions of the reactions follows a pseudo-first-order kinetics. The apparent rate constant calculated from the slopes of the lines is shown in Table 2.

Table 2. The rate constant of reaction at different initial dye concentrations.

$[AO7]_0$ (mg L^{-1})	75	100	125	150	175
R^2	0.901	0.901	0.902	0.883	0.924
P	1.67	0.95	0.47	0.36	0.16
k_{app} (min^{-1})	0.017	0.021	0.024	0.026	0.034

4. Conclusion

The AO7 wastewater was feasibly decolorized by either nZVI reduction or the nZnO-P photooxidation process. The reduction by nZVI-P for dye solution obtained better decolorization than mineralization. However, once the nZVI-P reduction is connected to the nZnO-P process, it can solve the above problem by eliminating TOC thoroughly for almost complete color reduction up to 67%. Consequently, 77% decolorization of dye bath effluent can be achieved by the nZVI-P system coupled with the nZnO-P process within 20 min. Thus, the experiments showed that the integrated process could be used as an efficient process for dye wastewater treatment. The kinetics analysis demonstrated that the removal of AO7 by the integrated system fits well with the pseudo-first-order reaction with respect to the dye concentration. It was also observed that the apparent reaction rate constant is independent of the initial dye concentration within the concentration range.

Acknowledgment

The authors thank the North Tehran Branch, Islamic Azad University, Iran, for the financial support given for this study.

Nomenclature:

AO7	Acid orange 7	TOC	Total organic carbon
nZnO-P	Nano ZnO immobilized on perlite	X	Degree of decolorization
nZVI-P	Nano zero-valent iron immobilized on perlite	ZVI	Zero-valent iron

References

Agrawal, A. and Tratnyek, P.G., "Reduction of Nitro Aromatic Compounds by Zero-Valent Iron Metal", Environmental Science and Technology, 30, 153–160, 1996.

Antoine, G., "Degradation of Benomyl, Picloram, and Dicamba in a Conical Apparatus by Zero-Valent Iron Powder", Chemosphere, 43, 1109–1117, 2001.

Bahnemann, W., Muneer, M. and Haque, M.M., "Titanium Dioxide-Mediated Photocatalysed Degradation of Few Selected Organic Pollutants in Aqueous Suspensions", Catalysis Today, 124, 133–148, 2007.

Chakrabarti, S. and Dutta, B.K., "Photocatalytic Degradation of Model Textile Dyes in Wastewater using ZnO as Semiconductor Catalyst", Journal of Hazardous Materials, 112, 269–278, 2004.

Chang, J.H. and Cheng, S.F., "The Remediation Performance of a Specific Electrokinetics Integrated with Zero-Valent Metals for Perchloroethylene Contaminated Soils", Journal of Hazardous Materials, 131, 153–162, 2006.

Chang, M.C., Shu, H.Y. and Yu, H.H., "An Integrated Technique using Zero-Valent Iron and UV/H_2O_2 Sequential Process for Complete Decolorization and Mineralization of C.I. Acid Black 24 Wastewater", Journal of Hazardous Materials, 138, 574–581, 2006.

Cheng, Y., Sun, H., Jin, W. and Xu, N., "Effect of Preparation Conditions on Visible Photocatalytic Activity of Titania Synthesized by Solution Combustion Method", Chinese Journal of Chemical Engineering, 15, 178–183, 2007.

Damodar, R.A. and Swaminathan, J.T., "Decolourization of Reactive Dyes by Thin Film Immobilized Surface Photoreactor using Solar Irradiation", Solar Energy, 81, 1–7, 2007.

Daneshvar, N., Aber, S., Khani, A. and Khataee, A.R., "Study of Imidaclopride Removal from Aqueous Solution by Adsorption onto Granular Activated Carbon Using an On-Line Spectrophotometric Analysis System", Journal of Hazardous Materials, 144, 47–51, 2007a.

Daneshvar, N., Aber, S., Khani, A. and Rasoulifard, M.H., "Investigation of Adsorption Kinetics and Isotherms of Imidacloprid as a Pollutant from Aqueous Solution by Adsorption onto Industrial Granular Activated Carbon", Journal of Food, Agriculture and Environment, 5, 425–429, 2007b.

Daneshvar, N., Rasoulifard, M.H., Khataee, A.R. and Hosseinzadeh, F, "Removal of C.I. Acid Orange 7 from Aqueous Solution by UV Irradiation in the Presence of ZnO Nanopowder", Journal of Hazardous Materials, 143, 95–101, 2007c.

Daneshvar, N., Salari, D. and Khataee, A.R., "Photocatalytic Degradation of Azo Dye Acid Red 14 in Water on ZnO as an Alternative Catalyst to TiO_2", Journal of Photochemistry and Photobiology A, 162, 317–322, 2004.

Devlin, J.F., Klausen, J. and Schwarzenbach, R.P., "Kinetics of Nitroaromatic Reduction on Granular Iron in Recirculating Batch Experiments", Environmental Science and Technology, 32, 1941–1947, 1998.

Erdem, T.K., Meral, Ç., Tokyay, M. and Erdoğan, T.Y., "Use of Perlite as a Pozzolanic Addition in Producing Blended Cements", Cement Concrete Composites, 29, 13–21, 2007.

Gong, W.J., Tao, H.W., Zi, G.L., Yang, X.Y., Yan, Y.L., Li, B. and Wang, J.Q., "Visible Light Photodegradation of Dyes Over Mesoporous Titania Prepared by Using Chrome Azurol S as Template", Research on Chemical Intermediates, 35, 751–762, 2009.

Hosseini, S.N., Borghei, S.M., Vossoughi, M. and Taghavinia, N., "Immobilization of TiO_2 on Perlite Granules for Photocatalytic Degradation of Phenol", Applied Catalysis B, 74, 53–62, 2007.

Hu, J., Lo, I.M.C. and Chen, G.H., "Fast Removal and Recovery of Cr(VI) Using Surface Modified Jacob Site ($MnFe_2O_4$) Nanoparticles", Langmuir, 21, 11173–11179, 2005.

Huang, C.P., Wang, H.W. and Chiu, P.C., "Nitrate Reduction by Metallic Iron", Water Research, 32, 2257–2264, 1998.

Kandavelu, V., Katien, H. and Thampi, R., "Photocatalytic Degradation of Isothiazolin-3-ons in Water and Emulsion Paints Containing Nanocrystalline TiO_2 and ZnO Catalysts", Applied Catalysis B, 48, 101–111, 2004.

Kanel, S.R., Manning, B., Charlet, L. and Choi, H., "Removal of Arsenic(III) from Groundwater by Nanoscale Zero-Valent Iron", Environmental Science and Technology, 39, 1291–1298, 2005.

Karri, S., Sierra-Alvarez, R. and Field, J.A., "Zero Valent Iron as an Electron-Donor for Methanogenesis and Sulfate Reduction in Anaerobic Sludge", Biotechnology and Bioengineering, 92, 810–819, 2005.

Kesraoui-Abdessalem, A., Oturan, N., Bellakhal, N., Dachraoui, M. and Oturan, M.A., "Experimental Design Methodology Applied to Electro-Fenton Treatment for Degradation of Herbicide Chlortoluron", Applied Catalysis B, 78, 334–341, 2008.

Khani, A., Sohrabi, M.R., Khosravi, M. and Davallo, M., "Decolorization of an Azo Dye from Aqueous Solution by Nano Zero-Valent Iron Immobilized on Perlite in Semi Batch Packed Bed Reactor", Fresenius Environmental Bulletin, 21, 2153–4170, 2012.

Khataee, A.R., Zarei, M., Fathinia, M. and Khobnasab Jafari, M., "Photocatalytic Degradation of an Anthraquinone Dye on Immobilized TiO_2 Nanoparticles in a Rectangular Reactor: Destruction Pathway and Response Surface Approach", Desalination, 268, 126–133, 2011.

Khodja, A.A., Sehili, T., Pilichowski, J. and Boule, P., "Photocatalytic Degradation of 2 Phenyl-Phenol on TiO_2 and ZnO in Aqueous Suspension", Journal of Photochemistry and Photobiology A, 141, 231–239, 2001.

Lin, Y.T. and Weng, C.H., "Effective Removal of AB24 Dye by Nano/Micro-Size Zero-Valent Iron", Separation and Purification Technology, 64, 26–30, 2008.

Machado, N.R.C.F. and Santana, V.S., "Influence of Thermal Treatment on the Structure and Photocatalytic Activity of TiO_2 P25", Catalysis Today, 107, 595–601, 2005.

Medina-Valtierra, J., Moctezuma, E., Sanchez-Cardenas, M. and Frausto-Reyes, C., "Global Photonic Efficiency for Phenol Degradation and Mineralization in Heterogeneous Photocatalysis", Journal of Photochemistry and Photobiology A, 174, 246–252, 2005.

Ponder, S.M., Darab, J.G. and Mallouk, T.E., "Remediation of Cr(VI) and Pb(II) Aqueous Solutions Using Supported, Nanoscale Zero-Valent Iron", Environmental Science and Technology, 34, 2564–2569, 2000.

Rahmani, A.R., Zarrabi, M., Samarghandi, M.R., Afkhami, A. and Ghaffari, H.R., "Degradation of Azo Dye Reactive Black 5 and Acid Orange 7 by Fenton-Like Mechanism", Iranian Association of Chemical Engineering, 7, 87–94, 2010.

Schrick, B., Blough, J.L., Jones, A.D. and Mallouk, T.E., "Hydrodechlorination of Trichloroethylene to Hydrocarbons using Bimetallic Nickel–Iron Nanoparticles", Chemistry of Materials, 14, 5140–5147, 2002.

Selvam, K., Muruganandham, M., Muthuvel, I. and Swaminathan, M., "The Influence of Inorganic Oxidants and Metal Ions on Semiconductor Sensitized Photodegradation of 4-Fluorophenol", Chemical Engineering Journal, 128, 51–57, 2007.

Shu H.Y., Chang, M.C. and Chang, C.C., "Integration of Nanosized Zero-Valent Iron Particles Addition with UV/H_2O_2 Process for Purification of Azo Dye Acid Black 24 Solution", Journal of Hazardous Materials, 167, 1178–1184, 2009.

Shu, H.Y., Chang, M.C., Yu, H.H. and Chen, W.H., "Removal of Di-Azo Dye Acid Black 24 in Synthesized Wastewater Using Zero-Valent Iron Nanoparticle", Journal of Colloid and Interface Science, 314, 89–97, 2007.

Xiong, Z., Zhao, D.Y. and Pan, G., "Rapid and Complete Destruction of Perchlorate in Water and Ion-Exchange Brine Using Stabilized Zero-Valent Iron Nanoparticles", Water Research, 41, 3497–3505, 2007.

Zhang, W.X., "Nanoscale Iron Particles for Environmental Remediation: An Overview", Journal of Nanoparticle Research, 5, 323–332, 2003.